![coatings logo]

MDPI

Communication

Reduction of Wall Friction of Fine Powders by Use of Wall Surface Coatings

Christof Lanzerstorfer *, Christian Forsich and Daniel Heim

School of Engineering, University of Applied Sciences Upper Austria, 4600 Wels, Austria;
christian.forsich@fh-wels.at (C.F.); daniel.heim@fh-wels.at (D.H.)
* Correspondence: c.lanzerstorfer@fh-wels.at; Tel.: +43-50804-43220

Abstract: In this study, the possibilities for the reduction of powder wall friction by different types of surface coatings on the wall material were investigated. Two conventional coatings, an ultra-high molecular weight polyethylene plate and an anti-friction varnish, were tested, together with a diamond-like carbon coating. It is the first time a diamond-like carbon coating has been researched with respect to powder wall friction reduction. The wall friction angles were measured with a ring-shear tester. The results showed that the conventional coatings did not really reduce wall friction in comparison to structural steel. In comparison to the stainless steel they even increased it. In contrast, the diamond-like carbon coating reduced wall friction significantly. These first results are very promising. However, more detailed investigations are required.

---

check for updates

1. Introduction

Wall friction is an important effect which has to be considered in the design and operation of powder conveying, dosing, and storage equipment. In most cases, low wall friction between the powder and the wall material is advantageous. Wall friction can be quantified by either the wall friction coefficient μ or the wall friction angle φ_W [1]. Both parameters can be calculated from the wall shear stress τ_W and the wall normal stress σ_W (Equations (1) and (2))

$$\mu = \frac{\tau_W}{\sigma_W} \tag{1}$$

$$\varphi_W = \arctan\left(\frac{\tau_W}{\sigma_W}\right) \tag{2}$$

Wall friction depends on the properties of both the powder particles and the wall material. Particle size is an important parameter with respect to wall friction. Larger wall friction angles for smaller particle sizes were reported for example for wet gypsum [2] and for fly ash from biomass combustion plants [3]. Additionally, other powder properties like the chemical composition of the powder, the shape and the hardness of the particles [1] as well as the moisture content of the powder [4] influence wall friction. However, the properties of the powder are mainly defined by the respective production process and means to reduce wall friction are usually limited to the selection of the wall surface material. An important wall material property for wall friction is the surface roughness of the wall. Larger friction angles were reported for higher values of the wall roughness for salt [5] as well as for polyethylene pellets [6] and limestone powder [7]. Other important parameters of the wall material are its hardness and its chemical composition [1].

The aim of the present study was to investigate the potential for the reduction of powder wall friction by using different types of coatings and comparing them to a structural steel sample and a stainless steel sample. As conventional coating materials, an ultra-high molecular weight polyethylene (PE-UHMW) plate and an anti-friction varnish, which are

both specified for use in bulk solids applications, were tested. Additionally, a diamond-like carbon (DLC) coating was investigated. Because of the outstanding properties of DLC such as a high degree of hardness, chemical inertness, low friction coefficients, and low-wear-rate DLC films can be widely used in different applications [8]. Therefore, DLC coatings on sliding parts find widespread applications for friction and wear reduction [9], for example for milling [10] and cutting tools [11], for plastic injection molds [12], for engine parts [13], and for push-fit joints [14].

In contrast, no literature could be found dealing with the influence of DLC films on wall friction of particulate materials.

2. Materials and Methods

A sample of structural steel S235JR and a sample of stainless steel 1.4301 were used as the basis for the comparison. Three different types of wall coating were investigated: firstly, a plate consisting of PE-UHMW (Robalon®-S [15]) which is used in bulk solids handling applications; secondly, the anti-friction varnish Agrovan 209 [16], an epoxy resin coating which is specified for use in bulk solids applications, and thirdly, a self-made diamond-like carbon (DLC) coating was tested. The anti-friction varnish was applied to a thickness of approximately 500 μm on a structural steel S235JR sample. The DLC coating was applied on a stainless steel 1.4301 sample. The film thickness of the a-C:H:Si coating was assessed using a self-made calotester with a ball of 25.4 mm diameter resulting in a thickness of approximately 20 μm.

The DLC coating consists of an amorphous hydrogenated carbon film. In order to modify its properties Si was embedded into the carbon matrix (a-C:H:Si). The coating was deposited on a stainless steel sample (1.4301) in a hot wall plasma-assisted chemical vapor deposition (PACVD) reactor (Rübig, Wels, Austria). The gas mixture consisted of acetylene, argon, and hexamethyldisiloxane regulated by mass flow controllers. Further information concerning the PACVD system has been published previously [17]. The chemical composition of the a-C:H:Si film was determined by using a SEM-EDX-detector (Oxford Instruments, Abingdon, UK), resulting in silicon content of approximately 25%.

The surface roughness of the wall samples was measured with a Mitutoyo SJ-201p surface roughness tester (Mitutoyo, Kawasaki, Japan) along two perpendicular axes. The instrument measures the one-dimensional surface roughness profile with a measuring feeler which scans the unevenness of the surface. The vertical displacement of the feeler pin is recorded and converted to the standardized output values R_a (arithmetical mean roughness value) and R_z (mean roughness depth).

The hardness of the a-C:H:Si film was measured by nanoindentation (Nano Indenter XP) with a Berkovich diamond tip (MTS, Eden Prairie, MN, USA) applying a maximum load force of 30 mN. The obtained HV-values were converted to GPa. The bulk hardness of the test wall materials (S235JR, stainless steel) was obtained by means of Vickers indentation (Gnehm Härteprüfer AG, Thalwil, Switzerland) according to EN ISO 6507 and also converted to GPa. The hardness of the PE-UHMW sample was measured with a Shore durometer (Zwick Roell, Ulm, Germany) according to DIN ISO 7619.

Microscopic images of the various wall samples were taken with a scanning electron microscope TESCAN, type MIRA3 (TESCAN ORSAY Holding, Brno, Czech Republic).

The wall friction measurements were performed using four different powders ranging from a mass median diameter d_{50} of 14 μm to 155 μm. The four powders were calcium carbonate (99.6% $CaCO_3$), quartz flour (>98% SiO_2), alumina (>99% Al_2O_3), and silica sand (100% < 0.25 mm).

The wall friction angle was determined using an RST-XS ring shear tester from Schulze (Dr. Dietmar Schulze Schüttgutmesstechnik, Wolfenbüttel, Germany). The bottom ring of the wall friction shear cell is formed by a sample of the wall material tested.

Figure 1 shows the sequences of a shear test. In the first step the wall sample is placed into the wall shear cell. In the second step the space above the wall sample is filled up to the top with the powder used in the test. Afterwards, the shear cell is mounted in the

annular shear tester and the lid is placed carefully onto the powder surface. Then the rod for the vertical load F_V and the two rods for the horizontal fixation of the lid are placed into position. During a test a certain wall normal stress is generated by the vertical load. The wall shear cell is rotated at a constant angular velocity ω while the lid is kept in position by the pair of horizontal forces F_H, which are measured for the calculation of the wall shear stress.

Wall shear cell with wall sample　　　　　　　Wall shear cell filled with powder
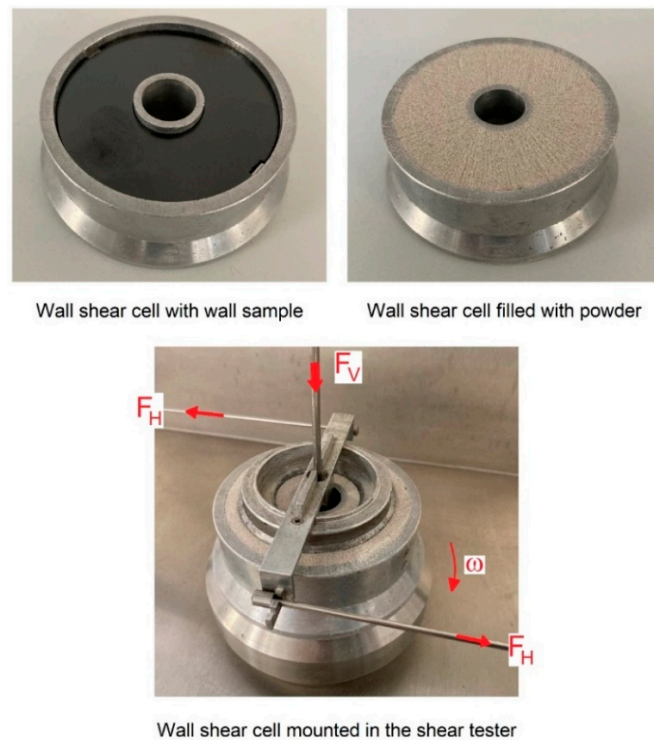
Wall shear cell mounted in the shear tester

Figure 1. Shear tester test sequence.

To obtain a point of the wall yield locus, corresponding pairs of values of the normal stress and the shear stress were determined. The kinematic angle of wall friction results from the slope of a straight line running through the origin of the σ-τ-diagram and a point of the wall yield locus [1]. The test procedure was performed at five values of the wall normal stress: 240 Pa, 600 Pa, 2000 Pa, 6000 Pa, and 20,000 Pa. Each measurement was repeated four to five times.

The particle size distribution of the powder samples was measured using a Sympatec HELOS/RODOS laser diffraction instrument (Sympatec, Clausthal-Zellerfeld, Germany) with dry sample dispersion. The calibration of the instrument was checked with a Sympatec SiC-P600′06 standard (Sympatec, Clausthal-Zellerfeld, Germany).

The moisture content of the powders was determined by drying at 105 °C.

3. Results

3.1. Wall Materials

The results of the surface roughness measurements of the tested wall materials are summarized in Table 1. The arithmetical mean roughness value R_a and the mean roughness depth R_z were very similar for the stainless steel and the DLC coating, which have the lowest surface roughness. The structural steel and the PE-UHMW have approximately twice the roughness. The highest values for the roughness were measured for the anti-friction varnish. Figure 2 shows microscopic images of the wall samples. After using the samples in the shear tests no damages of the coatings were visible.

Table 1. Wall materials used in the wall friction tests.

Wall Material	R_a in μm [1]	R_z in μm [2]	Hardness
S235JR	1.03	5.6	1.4 GPa
Stainless steel 1.4301	0.46	3.3	1.5 GPa
PE-UHMW	1.04	6.5	65.2 Shore D
Agrovan 209 coating	2.52	14.6	-
DLC coating	0.51	3.1	10.2 GPa

[1] R_a Arithmetical mean roughness value; [2] R_z Mean roughness depth.
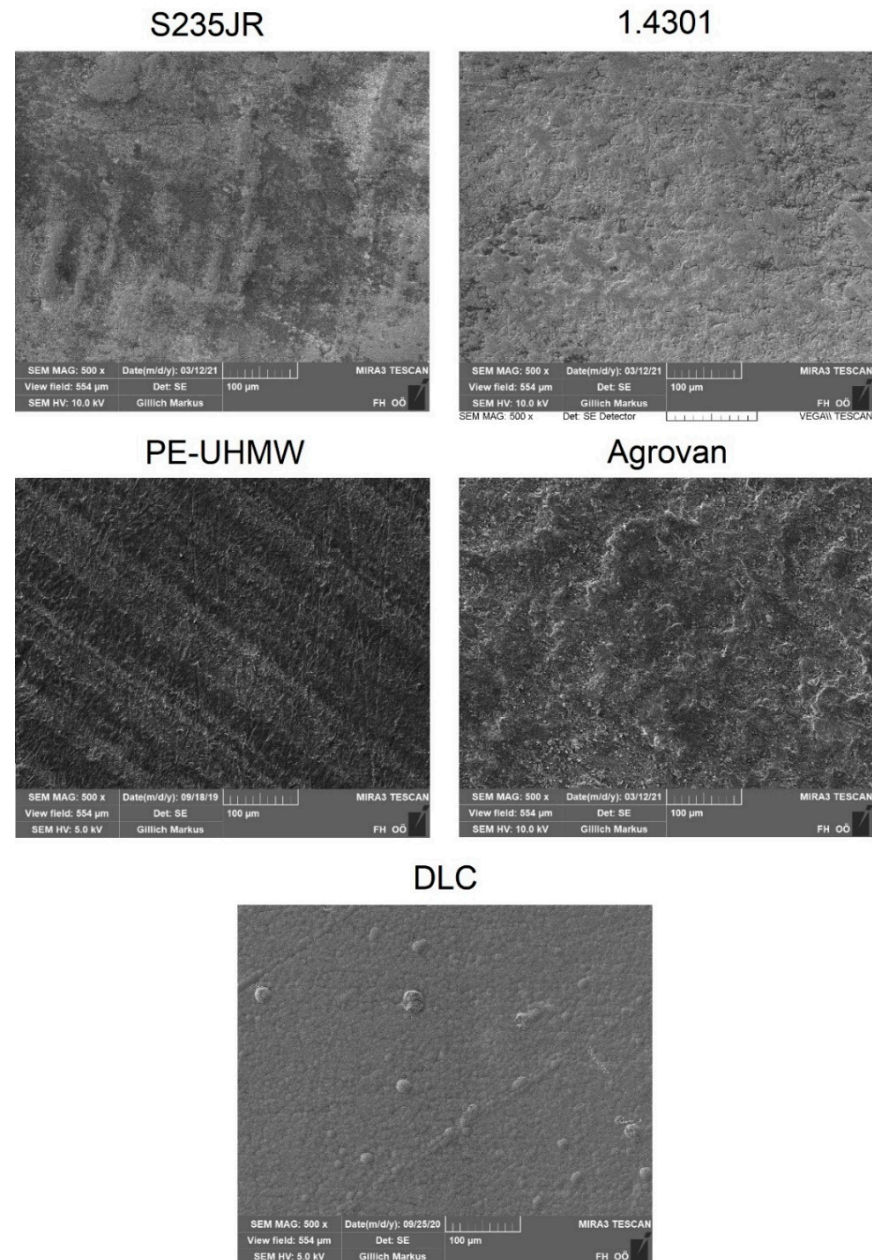
**Figure 2.** Microscopic images of the wall samples.

3.2. Powder Materials

The powder samples and their particle size data are summarized in Table 2. The particle size distributions of the powder samples are shown in Figure 3.

Table 2. Powder samples used in the wall friction tests

Powder Material	d_{50} in μm [1]	Moisture Content in %
$CaCO_3$	14	0.15
SiO_2	29	0.22
Al_2O_3	88	0.98
Silica sand F38	155	0.06

[1] d_{50} Mass median diameter.
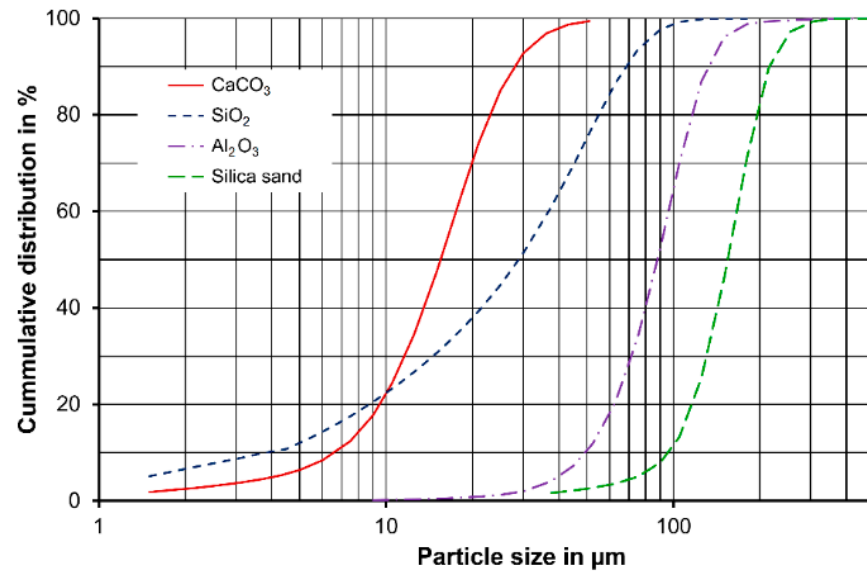
Figure 3. Particle size distribution of the powder samples.

3.3. Wall Friction Angles

The results of the wall friction angle measurements for the four different powders are summarized in Figure 4. In the diagrams the average wall friction angles and the standard deviations are shown for different values of the wall normal stress. Generally, the wall friction angles decreased with increasing wall normal stress. The effect of lower values for the wall friction angle at higher values of the wall normal stress was reported previously [18]. The strength of this effect varied greatly, depending on the wall surface material and the type of powder.
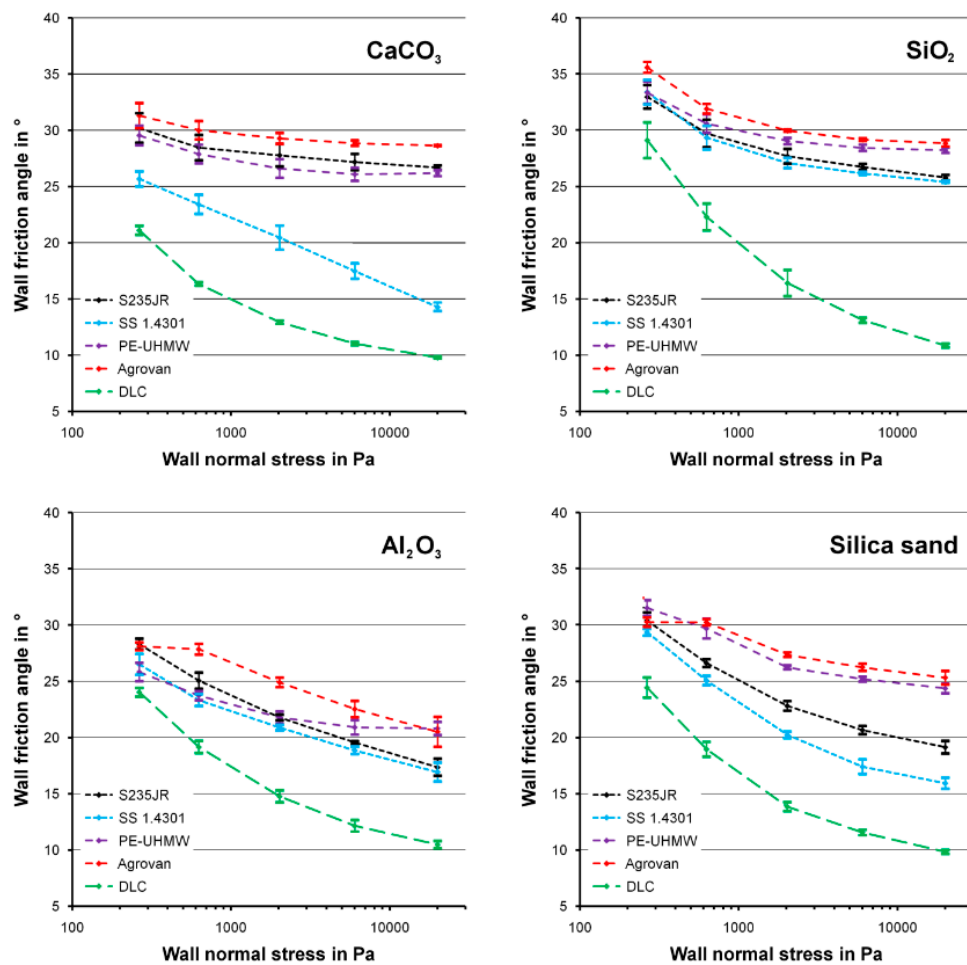
Figure 4. Wall friction angle for various wall materials as a function of the wall normal stress.

4. Discussion

Generally, the wall materials can be ranked as follows with regard to decreasing wall friction: anti-friction varnish > PE-UHMW plate > structural steel S235JR > stainless steel 1.4301 > DLC coating.

The wall friction angles with the stainless steel 1.4301 were always smaller than with the structural steel S235JR. The difference was mostly $0.5°-3°$, only for the finest powder (CaCO$_3$) was the difference much higher ($5°-13°$). This difference might partly explained by the higher values of the wall roughness of the structural steel [5–7].

The conventional coating materials, the PE-UHMW plate and the anti-friction varnish did not reduce wall friction. In contrast, the wall friction angles with the anti-friction varnish were the highest in nearly all cases and the wall friction angles with the PE-UHMW plate were slightly smaller. Although this difference fits to the reported relation between powder wall friction and surface roughness [5–7]. For the three finer powder samples the wall friction with the PE-UHMW plate and the structural steel was similar, while for the coarser silica sand the wall friction with the steel sample was significantly less.

The wall friction angles with the DLC coating were in all cases smaller. In comparison to the wall friction angles with the stainless steel sample, the reduction was between $2°$ and $14°$.

5. Conclusions

This study showed that conventional coatings like the PE-UHMW plate and the anti-friction varnish do not really reduce wall friction in comparison to the wall friction with structural steel, while in comparison to the stainless steel the conventional coatings even

increased wall friction. In contrast, the DLC coating reduced the wall friction angles of the powders significantly. These first results are very promising. Nevertheless, further research is required to clarify how wall friction of powders is reduced by the DLC coating.

References

1. Schulze, D. *Powders and Bulk Solids—Behavior. Characterization. Storage and Flow*; Springer: Berlin, Germany, 2008; pp. 69–74, 243–247.
2. Schulze, D.; Schwedes, J. Das Fließverhalten und die Silolagerung von REA-Gips. *Chem. Ing. Tech.* **1991**, *63*, 256–257. [CrossRef]
3. Lanzerstorfer, C. Characterization of the flowability of fly ashes from grate-fired combustion of forest residues. *Fuel Proc. Technol.* **2016**, *150*, 10–15. [CrossRef]
4. Iqbal, T.; Fitzpatrick, J.J. Effect of storage conditions on the wall friction characteristics of three food powders. *J. Food Eng.* **2006**, *72*, 273–280. [CrossRef]
5. Heinrici, H. Wie lassen sich Siloschäden vermeiden? In *Schüttgut Fördern und Lagern, VDI Bericht 1918*; VDI, Ed.; VDI-Verlag: Düsseldorf, Germany, 2006; pp. 117–130.
6. Han, T. Comparison of wall friction measurements by Jenike shear tester and ring shear tester. *KONA Powder Part. J.* **2011**, *29*, 118–124. [CrossRef]
7. Lanzerstorfer, C. Influence of the surface roughness of grit-blasted steel on the wall friction angle of limestone powder. In Proceedings of the 14th Minisymposium Verfahrenstechnik, Linz, Austria, 4–5 April 2018; pp. 1–4.
8. Meng, Y.; Xu, J.; Jin, Z.; Prakash, B.; Hu, Y. A review of recent advances in tribology. *Friction* **2020**, *8*, 221–300. [CrossRef]
9. Donnet, C.; Erdemir, A. New horizon in the tribology of diamond like carbon films. *Surf. Eng.* **2008**, *24*, 399–401. [CrossRef]
10. Fuß, H.-G. Industrial Production of DLC Coatings. In *Tribology of Diamond-Like Carbon Films. Fundamentals and Applications*; Donnet, C., Erdemir, A., Eds.; Springer: New York, NY, USA, 2008; pp. 457–468.
11. Björling, M.; Isaksson, P.; Marklund, P.; Larsson, R. The Influence of DLC Coating on EHL Friction Coefficient. *Tribol. Lett.* **2012**, *47*, 285–294. [CrossRef]
12. Héau, C. DLC Films in Mechanical and Manufacturing Industry. In *Tribology of Diamond-Like Carbon Films. Fundamentals and Applications*; Donnet, C., Erdemir, A., Eds.; Springer: New York, NY, USA, 2008; pp. 469–483.
13. Gangopadhyay, A.; Sinha, K.; Uy, D.; McWatt, D.G.; Zdrodowski, R.J.; Simko, S.J. Friction, Wear, and Surface Film Formation Characteristics of Diamond-Like Carbon Thin Coating in Valvetrain Application. *Tribol. Trans.* **2011**, *54*, 104–114. [CrossRef]
14. Kowalski, S. Analysis of the possibilities of using CrN+a-C:H:W coatings to mitigate fretting wear in push fit joints operating in rotational bending conditions. *Tribologia* **2018**, *277*, 45–55. [CrossRef]
15. Röchling. Robalon®-S. 2021. Available online: https://www.roechling.com/industrial/materials/thermoplastics/detail/robalon-s-3142 (accessed on 26 March 2021).
16. Avenarius Agro. Agrovan 2009. 2021. Available online: https://www.avenariusagro.at/produkt/anstrichstoffe-/\deckbeschichtungen-2k/agrovan-209 (accessed on 27 February 2021).
17. Forsich, C.; Dipolt, C.; Heim, D.; Mueller, T.; Gebeshuber, A.; Holecek, R.; Lugmair, C. Potential of thick a-C:H:Si films as substitute for chromium plating. *Surf. Coat. Technol.* **2014**, *24*, 86–92. [CrossRef]
18. Lanzerstorfer, C. Consideration of the stress dependence of the bulk density in silo storage of dusts from dry off-gas cleaning. *Adv. Powder Technol.* **2017**, *28*, 115–121. [CrossRef]